CONF-870812--22

Cladding Failure Margins for Metallic Fuel in the Integral Fast Reactor

by

T. H. Bauer[1], G. R. Fenske[2], and J. M. Kramer[1]

Argonne National Laboratory
9700 South Cass Avenue
Argonne, Illinois 60439

CONF-870812--22

DE87 011460

1. Introduction

The Integral Fast Reactor (IFR) concept being developed at Argonne National Laboratory has prompted a renewed interest in uranium-based metal alloys as a fuel for sodium-cooled fast reactors. One of the key features of metallic fuel is improved inherent safety through lower stored energy and enhanced negative reactivity feedback response during normal and off-normal transients. Part of the effort in demonstrating inherent safety for IFR involves the establishment of margins-to-failure for metallic fuel during these transient events.

The reference fuel for IFR is a ternary U-Pu-Zr alloy with a low swelling austenitic or ferritic stainless steel cladding. It is known that low melting point eutectics may form in such metallic fuel-cladding systems which could contribute to cladding failure under accident conditions. In this paper we will present recent measurements of cladding eutectic penetration rates for the ternary IFR alloy and will compare these results with earlier eutectic penetration data for other fuel and cladding materials. A method for calculating failure of metallic fuel pins is developed by combining cladding deformation equations with a large strain analysis where the hoop stress is calculated using the instantaneous wall thickness as determined from correlations of the eutectic penetration-rate data. This method is applied to analyze the results of in-reactor and out-of-reactor fuel pin failure tests on uranium-fissium alloy EBR-II Mark-II driver fuel. In the final section of

[1] Reactor Analysis and Safety Division.
[2] Materials and Components Technology Division.

this paper we extend the calculations to consider the failure of IFR ternary fuel under reactor accident conditions.

2. Previous Eutectic Penetration-Rate Data

Most of the data base for cladding eutectic penetration is from out-of-reactor tests which measured the erosion of iron samples dipped into various iron-uranium melts [1]. This data, shown on an Arrhenius plot in Fig. 1, agrees with earlier dipping test data using uranium-fissium fuel and stainless steel cladding. The dipping test results indicate that the penetration rates are governed by iron and uranium phases and are relatively independent of the fuel or cladding alloy. The data show that the penetration rate $\dot{r}$ can be correlated to the absolute temperature T (in Kelvins) by

$$\dot{r} = \exp\ (22.847 - 27624/T),\ \mu m/s, \qquad (1)$$

except in the range of 1080 to 1233°C where

$$\dot{r} = 922 + 2.9765\ (T-1388) - 0.21522\ (T-1388)^2 \qquad (2)$$

$$+\ 0.0011338\ (T-1388)^3.$$

The accelerated penetration in the regime has been attributed to the breakdown of a protective UFe_2 layer that forms between the liquid and the cladding [1]. Below about 715°C the melting rate is zero because liquid phases do not form.

Results of tests where irradiated uranium-fissium EBR-II driver pins with stainless steel cladding were heated in a furnace [2,3] are also shown in Fig. 1. The apparent penetration rates were calculated from measured rupture times by using the methodology discussed in Section 4 of this paper. These results, along with the one data point where the actual penetration was measured prior to failure, agree well with the dipping test data.

Additional data for EBR-II driver pins from the in-reactor XY-22 eutectic penetration tests [4] are also shown in Fig. 1. In these tests fuel pins with burnups between 0.0 and 7.7 a/o were irradiated for 42 minutes at elevated cladding temperatures of around 800°C. Measured penetration rates are seen in the figure to be somewhat less than those from the dipping tests. In the XY-22 experiment the penetration was observed to decrease with increasing burnup. This may be due to gas bubbles as other fission products which form at the interface between the fuel and the cladding [4].

3.0 U-Pu-Zr Eutectic Interaction Experiments

Recently, U-Pu-Zr IFR fuel irradiated to ~ 2 at.% peak burnup has become available for transient testing. Experiments utilizing the out-of-reactor Direct Electrical Heating apparatus (DEH) have been performed to measure rates of cladding penetration for these ternary alloys.

3.1 Experimental Technique

The eutectic interaction behavior between irradiated U-19Pu-10Zr fuel and D9 stainless steel cladding was determined from post-test metallographic examination of short (~0.6-cm.) segments of EBR-II pins that were subjected to either steady-state or transient thermal histories in the DEH apparatus at ANL. The samples were placed inside of tantalum cups which in turn were surrounded by concentric, gas-tight quartz tubes. A thermocouple attached to the Ta cup monitored the temperature during each run. The cup with the sample inside was heated using an external infrared-heater that surrounded the quartz-tubes. High-purity helium flowed through the quartz-tubes and past the Ta-cup and sample to insure a non-reactive environment was present during the tests.

During the steady-state tests, the samples were first brought to a pre-test temperature of 200°C then ramped to the desired temperature (between 800- and 1100°C) at 75°C/s and held there for 5-min (the 110°C run only lasted 2.2 min.) before turning power to the furnace off. The transient runs were initiated at a pre-test temperature of 200°C and were heated at 15°C/s to a pre-determined temperature (1000 to 1120°C) at which time power to the

external heater was turned off.

3.2 Results

Figure 2 illustrates the type of microstructure that develops in the U-19Pu-10Zr alloy after irradiation in EBR-II to a peak burnup of 2.1 at.%. The most striking feature of the microstructure is the development of a ring structure, although in this case the intermediate ring is "tear-drop" shaped with the tip of the drop adjacent to the cladding. The intermediate zone has been identified as a Zr-deficient/U-enriched form of the original alloy with a solidus approximately 200°C lower than the starting alloy. As a result of the tear drop, the cladding actually sees two different fuel alloys adjacent to it during the test: one alloy is more representative of the starting alloy with a Zr content near 10%, while the tear drop alloy is deficient in Zr (approx. 2%Zr).

Figure 3 shows a composite micrograph of a segment of fuel similar to that shown in Fig. 2 that was heated to 1080°C at 15°C/s. It is obvious that the interaction rate between the fuel and the cladding depends on the type of fuel adjacent to the cladding during the transient. The region of cladding that originally had high-Zr fuel next to it interacted much less than the region that had low-Zr fuel adjacent to it.

Although the low-Zr fuel interacts with the cladding at a faster rate than the high-Zr fuel, the rate of interaction for the low-Zr fuel does not appear to be significantly higher than that for the U/Fe system used in the dipping tests. This is illustrated in Table I where the measured maximum depth of penetration is compared with the calculated penetration depth for a number of steady-state and transient runs on U-19Pu-10Zr pin segments. The calculated penetration was derived from Eqs. 1 and 2 using the actual temperature history of each run. The rate of penetration for the steady-state DEH tests is also shown in Fig. 1 along with the correlation and with the data for EBR-II driver fuel. Again, the ternary alloy penetration rate does not appear to be significantly different from that for the U-5Fs/316-SS system.

4. Calculation of Cladding Failure for Metallic Fuel Pins

Certain characteristics of metallic fuel pins simplify the analysis of cladding failure during transient events. High fuel conductivity leads to cladding temperatures that peak near the top of the pins. Here the primary cladding loading is the plenum pressure; the similarity of the fuel and the cladding thermal expansion, and the compliance of the fuel, lead to negligible fuel-cladding mechanical interaction.

For peak plenum pressure loadings at end of life of about 10 MPa, the primary mode of cladding mechanical failure during transient overheating is creep rupture. Under these same conditions eutectic penetration may erode the cladding wall. It appears, however, that the effect is only that of wall-thinning and does not include additional damage mechanisms such as liquid metal embrittlement. We have modeled cladding failure by calculating the deformation of a thin-walled cylinder whose wall thickness is continuously decreasing by plastic deformation and by eutectic attack. Equations 1 and 2 are used to determine the eutectic penetration rate. The deformation of the cladding tendon is determined from correlations for cladding plastic deformation which have been validated using data from transient burst tests. Failure is based on the total diametral strains measured in the burst tests.

The above methodology was used to analyze the furnace tests on irradiated EBR-II pins whose plenum pressures ranged from 0.5 and 15 MPa. Apparent penetration rates were determined so that the measured and calculated failure times agreed. As shown in Fig. 1, these penetration rates are consistent with the dipping test data. Similar calculations have also been performed for recent in-reactor TREAT overpower tests on irradiated EBR-II fuel pins. Agreement between predicted and measured failure times in these experiments [5] further supports the eutectic-penetration-enhanced creep-rupture model for transient failure of metallic fuel pins.

Figures 4 and 5 illustrate model predictions for failure of D9 austenitic cladding and HT-9 ferritic cladding with a constant plenum pressure of 10 MPa and a step increase in temperature. The thermal conditions approximate the inherent response of metal-fueled fast reactors to unprotected overpower and undercooling events where there is an initial rapid increase in cladding

temperature followed by an extended period of nearly constant temperature as the system equilibrates. The three curves show failure times considering creep rupture only, eutectic penetration only and combined creep plus eutectic penetration. The transient failure of D9-clad IFR pins under these conditions is apparently controlled by the eutectic penetration rate. On the other hand, HT-9 is creep-limited except for short times where the $\alpha \rightarrow \gamma$ phase transformation over the temperature range 850 to 950°C initially increases the cladding creep resistance. At temperatures below which liquid phases form at the fuel-cladding interface (about 715°C) the liquid penetration rate is zero and failure for both D9 and HT-9 is by creep rupture of the full wall thickness.

Similar calculations to those outlined above have been carried out for a variety of accident initiators. Cladding temperatures have been obtained from whole-core analyses of the accident events. In all cases studied, the metal-fueled IFR system offers wide margins to fuel pin failure.

5. Conclusions

The eutectic interaction behavior between irradiated U-19Pu-10Zr fuel and D9 cladding has been determined. Measured penetration rates are similar to those determined from earlier iron-uranium dipping tests and from out-of-reactor and in-reactor tests on stainless steel-clad uranium-fissium EBR-II pins. A correlation has been developed to relate the penetration rate to the fuel-cladding interface temperature. Calculations indicate that transient failure of IFR fuel pins can be predicted by considering creep rupture of the cladding under plenum pressure loading with the instantaneous wall thickness decreased by the amount of eutectic penetration. Failure of D9 clad IFR pins under end-of-life conditions is governed by the eutectic penetration rate whereas failure of HT-9 clad pins is governed by the creep strength.

Acknowledgements

The authors would like to thank Ms. Lois Miller for preparing the manuscript.

Work supported by the U.S. Department of Energy, Office of Technology Support Program, under Contract W-31-109-Eng-38.

References

[1] C. M. Walter and L. R. Kelman, "The Interaction of Iron with Molten Uranium", J. Nucl. Mat., 20, 314 (1966).

[2] P. R. Betten, J. H. Bottcher, and B. R. Seidel, "Eutectic Penetration Times in Irradiated EBR-II Driver Fuel Elements", Trans. Am. Nucl. Soc., 45, p. 300 (1983).

[3] B. R. Seidel, "Metallic Fuel Cladding Eutectic Formation During Postirradiation Heating", Trans. Am. Nucl. Soc., 34, p. 210 (1980).

[4] C. E. Lahm, J. F. Koenig, P. R. Betten, W. K. Lehto, and B. R. Seidel, "EBR-II Driver Fuel Qualification for Loss of Flow and Loss of Heat Sink Transients Without Scram", accepted for publication in Nuclear Engineering and Design.

[5] A. E. Wright, T. H. Bauer, R. K. Lo, W. R. Robinson, and R. G. Palm, "Recent Metal Fuel Tests in TREAT", Proceedings of the BNES/ENS/ANS Conference on Science and Technology of Fast Reactor Safety, Guernsey, 11-16 May 1986.

[6] R. G. Palm and D. J. Dever, Personal Communication, 1986.

Table I

Calculated and Measured Attack for U-19Pu-10Zr Fuel and D9 Cladding

Run Number	Test Temperature (°C)	Time at Temperature (s)	Calculated Attack (Microns)	Maximum Measured Attack (Microns)
Steady-State Tests				
IFR86-66	800	300	18.0	13.0
IFR86-56	920	300	215.0	51.0
IFR86-59	975	300	615.0	127.0
IFR86-54	1000	300	947.0	203.0
IFR86-53	1020	300	1330.0	Not Measured
IFR86-55	1100	130	1990.0	>381.0
Transient Tests				
IFR86-65	1000	N/A	25.0 - 33.0[1]	20.0
IFR86-64	1060	N/A	81.0 - 97.0	127.0
IFR86-63	1080	N/A	114.0 - 127.0	191.0
IFR86-58	1080	N/A	102.0 - 114.0	140.0
IFR86-60	1110	N/A	229.0 - 254.0	254.0

[1]Range of calculated attack reflects uncertainties [6] determining transient fuel temperatures from Ta cup thermocouple readings.

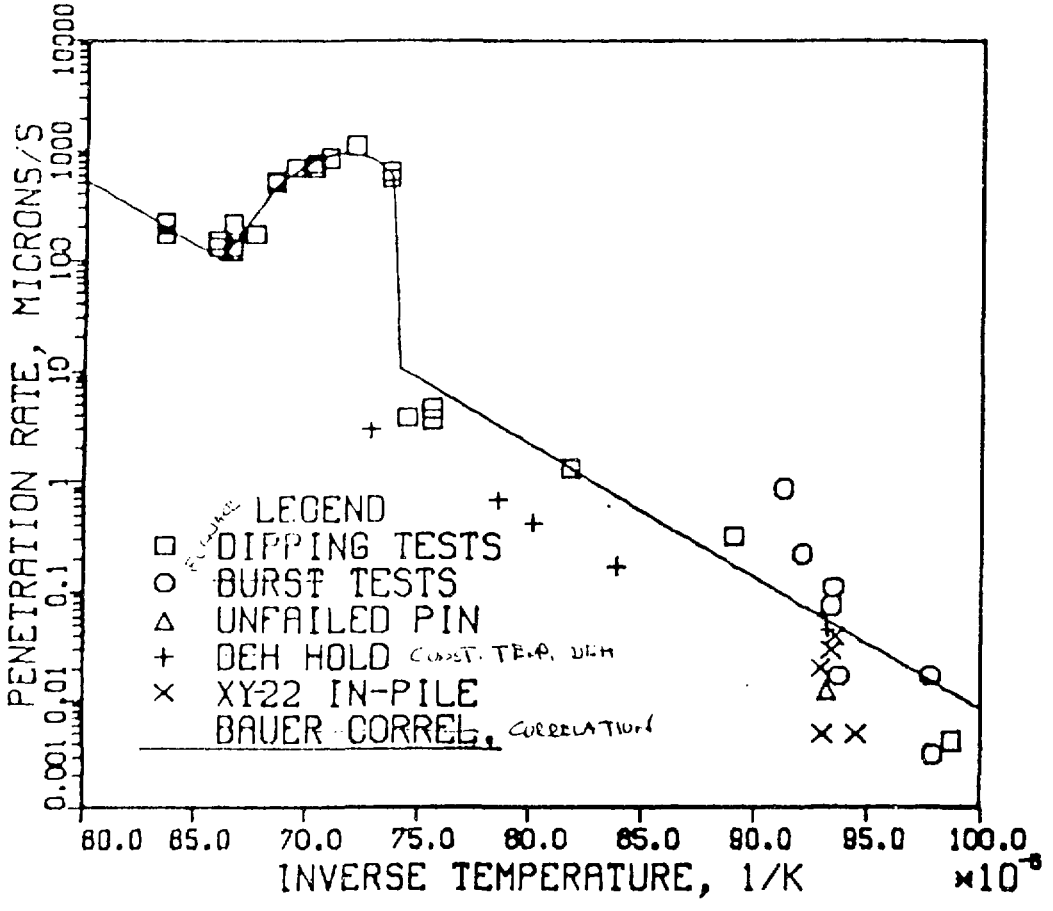
PENETRATION RATE, MICRONS/S
0.001
0.01
0.1
1
10
100
1000
10000
LEGEND
DIPPING TESTS
BURST TESTS
UNFAILED PIN
DEH HOLD
XY-22 IN-PILE
BAUER CORREL.
60.0
65.0
70.0
75.0
80.0
85.0
90.0
95.0
100.0
INVERSE TEMPERATURE, 1/K
×10⁻⁶

Figure 1

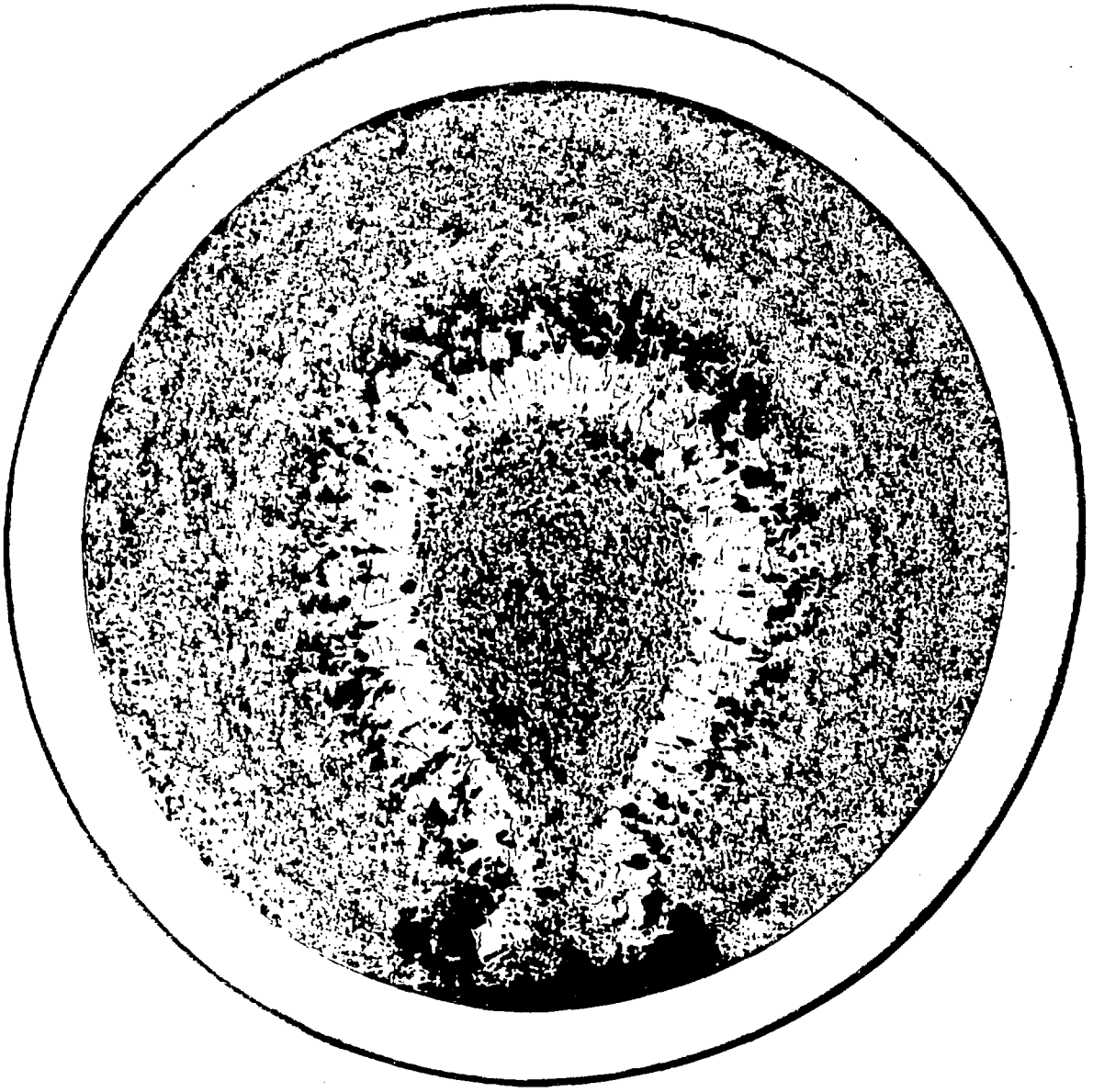

Figure 2

Figure 3

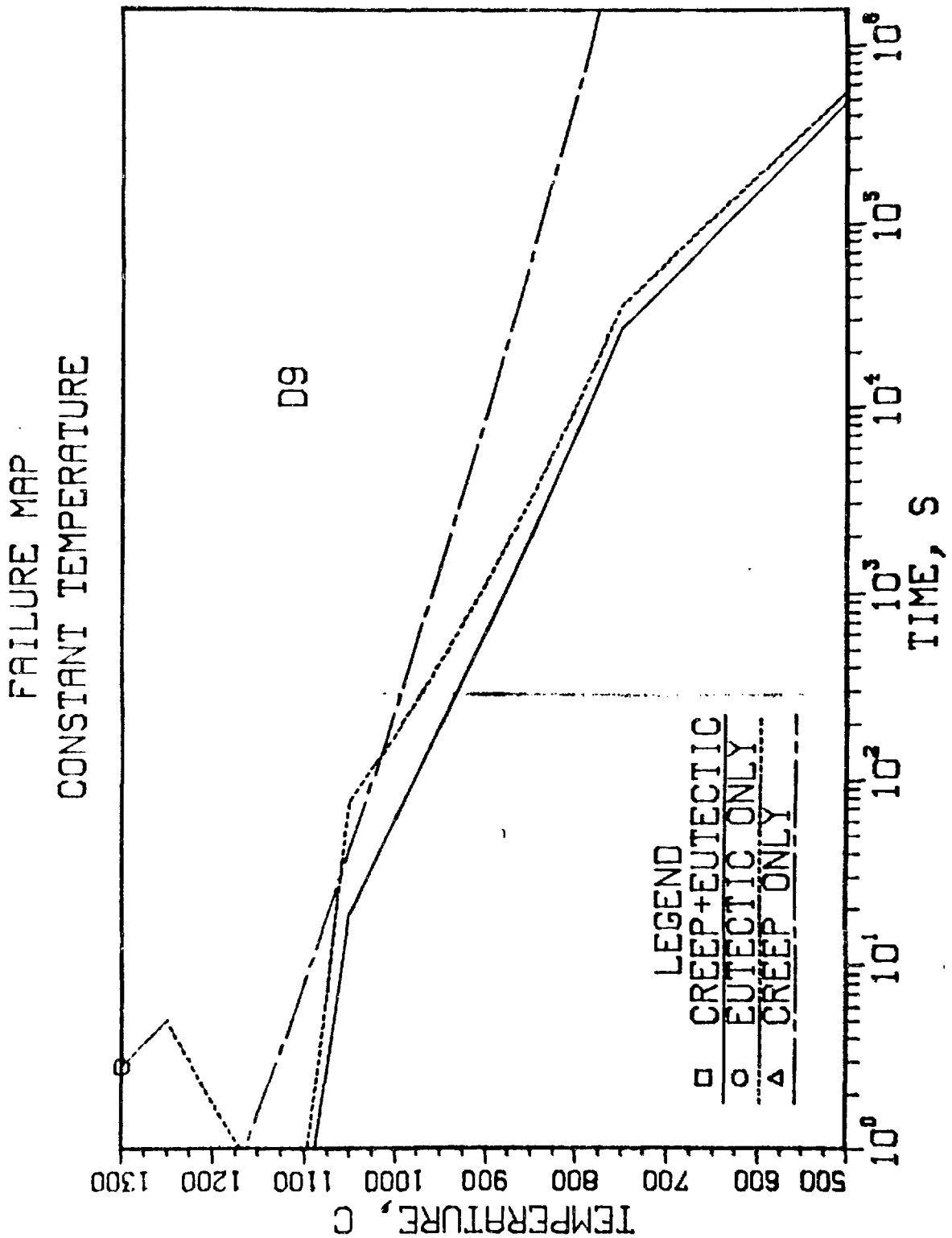
FAILURE MAP
CONSTANT TEMPERATURE
D9
LEGEND
□ CREEP+EUTECTIC
○ EUTECTIC ONLY
△ CREEP ONLY
TEMPERATURE, C
500
600
700
800
900
1000
1100
1200
1300
TIME, S
10^0
10^1
10^2
10^3
10^4
10^5
10^6

Figure 4

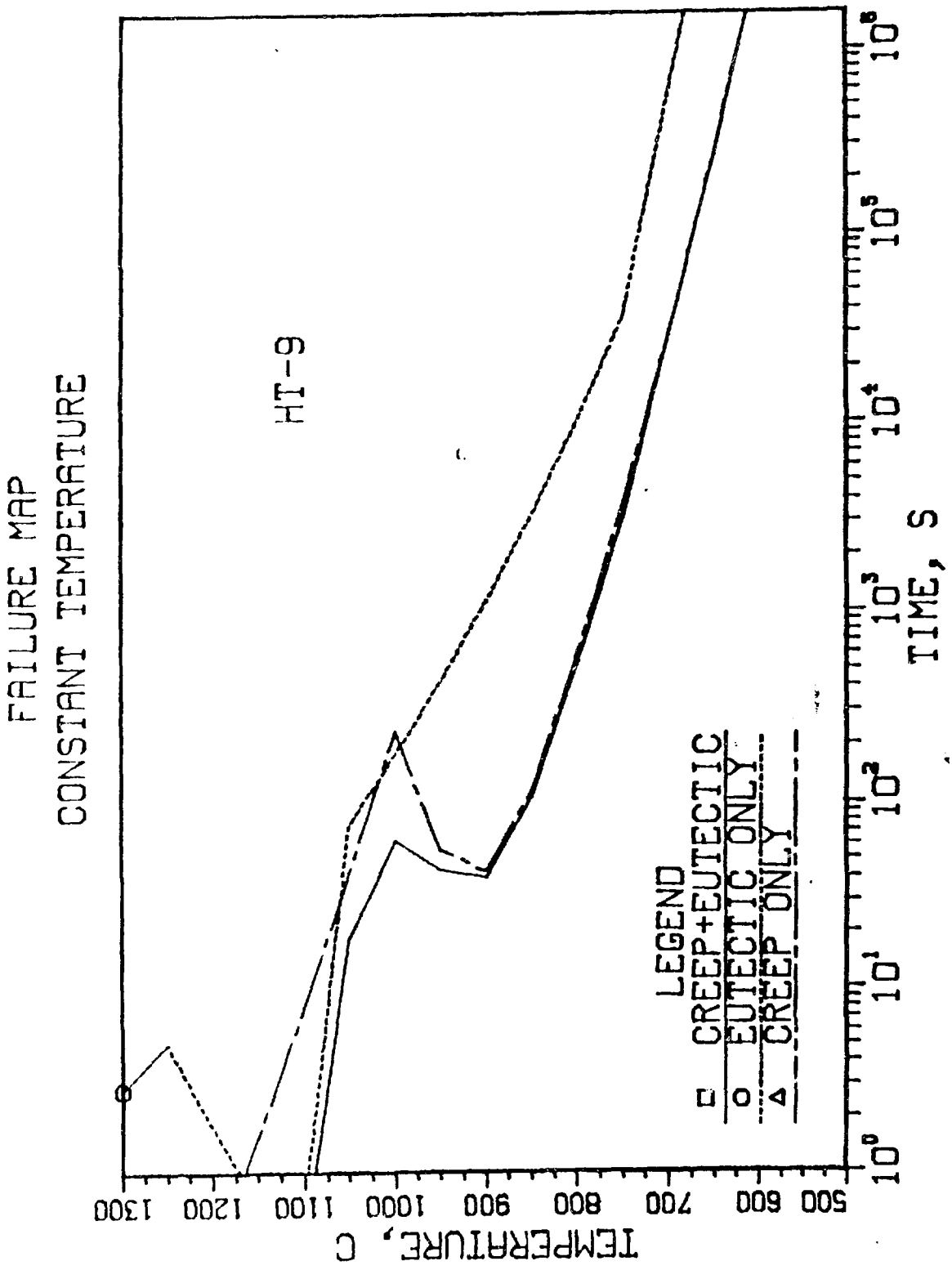
FAILURE MAP
CONSTANT TEMPERATURE
HT-9
LEGEND
□ CREEP+EUTECTIC
○ EUTECTIC ONLY
△ CREEP ONLY
TEMPERATURE, C
500 600 700 800 900 1000 1100 1200 1300
TIME, S
10^0 10^1 10^2 10^3 10^4 10^5 10^6

Figure 5

LIST OF FIGURES